



AME0012

Design of optimum contra-rotating propellers under slipstream contraction condition

Nattanun Subsamar^{*}, Chirdpun Vitooraporn

Mechanical Engineering Department, Chulalongkorn University, Bangkok, 10330, Thailand

* Corresponding Author: Nattanun.S@student.chula.ac.th

Abstract. The optimum design of contra-rotating propellers (CRPs) is needed to achieve the good improvement on ship propulsion efficiency. In this study, the lifting line theory and calculus of variation method are used to find an optimum CRPs blade profile under given condition. In real situation, the size of slipstream behind propeller decreases in order to conserve the mass flow rate as the velocity increases. This affects the induced velocities on propeller especially in CRPs where the interaction between two propellers is highly concerned. Therefore, the effect of slipstream contraction is included in this study. Equations obtained from calculus of variation method are solved numerically by using MATLAB. The optimum blade profile resulted from calculation is drawn and simulated in CFD program (ANSYS Fluent) to validate the obtained results.

1. Introduction

The design procedure of CRPs was developed from single propeller design. The analytic method for studying the propeller began with actuator disk theory, then blade element theory, lifting line, and lifting surface theory were developed consequently. Lerbs[1] studied the single propeller by using the lifting line theory and used the Betz condition and normal condition to find the optimum propeller's design. Lerbs[2] also applied the design method of single propeller for CRPs design by neglecting mutual-induced velocity that caused by the interaction between two propellers. He then used correction factors to correct the result later. Gunsteren[3] also used the lifting line theory to design the CRPs but assumed that the average value of mutual-induced velocities distributing along the blade is equal to the average mutual-induced velocity that determined from the momentum theory. Caster and LeFone[4] made the computer program for designing CRPs based on lifting line theory while mutual-induced velocity in program was obtained from Kerwin's field point program which is based on lifting surface theory. Corney[5] studied the method to find the optimum design for various types of ship propulsion including CRPs by applying the calculus of variation method with the lifting line theory. Laskos[6] studied optimum CRPs design by using the lifting line theory and calculus of variation method from Corney's study. In Laskos' study, the aft propeller's diameter was set to equal to the fore propeller's diameter and assumed that there was no slipstream contraction in the flow occurred behind each propeller. In this study, a further investigation for optimum CRPs from Laskos's study is done by including slipstream contraction effect which affects not only self and mutual-induced velocities but also the loads on propeller's blade itself. To simplify the calculation, the viscous effect is neglected. In order to recover the rotational loss in slipstream behind the fore propeller, the aft propeller's diameter is varied to correspond to the size of slipstream contraction during calculation. The slipstream

contraction model used in this study is obtained from Hoshino's study[7] which used LVD to measure the slipstream radius of single propeller in open water test. Results from calculation which are the circulation distributions of two propellers are then used to design the actual propeller' blade profiles by following Abbot and Doenhoff's study[8]. Obtained CRPs are drawn and simulated by using CFD program; Ansys FLUENT to verify calculation results.

2. Background theory

2.1 Lifting line theory

Each blade of propeller is replaced by straight line called lifting line in order to determine the propeller's performance. Along this lifting line, there are circulations distributing on it called bound vortex (Γ) which represent loads that occur on each blade sections. The variation of bound vortex circulation causes the free trailing vortex (Γ_f) shed in downstream. Its direction must align with the direction of flow velocity at the point that it leaves the lifting line. The shape of free trailing vortex line is like helix line and extends to infinity as shown in figure 1. The angle between free trailing vortex line and plane that perpendicular to rotational axis is called the pitch angle (β_0)

According to Biot-Savart law, the bound and free trailing vortices cause induced velocity at any point in the flow field. The induced velocity at each point on lifting line with the corresponding bound vortex is used to determine thrust and torque on that lifting line by using Kutta-Joukowski's theorem.

In order to apply the numerical method, the lifting line of each propeller is divided equally into finite elements as shown in figure 1. Each element consists of one control point in the middle and one vortex points at each of two ends. Circulation of bound vortex is placed at each control point, while the point for free trailing vortex shed in downstream is placed at the vortex point.

For contra-rotating propeller, induced velocities are separated into two parts, self-induced velocity and mutually-induced velocity in which one is induced by propeller itself and the other is by the other propeller in the CRPs set respectively. Following Kutta-Joukowski's theorem and neglecting the viscous force, thrust and torque on each propeller are found in equation(1) and (2).

$$T = \rho Z \sum_{i=1}^n [V_a + u_{a,s}(i) + u_{a,m}(i)] \Gamma(i) \Delta r \quad (1)$$

$$Q = \rho Z \sum_{i=1}^n [\omega r(i) + u_{t,s}(i) + u_{t,m}(i)] \Gamma(i) r(i) \Delta r \quad (2)$$

The self-induced velocity of propeller is determined by using Biot-Savart law as shown in equation(3) to (5). For free trailing vortex which has constant radius and constant pitch angle, the integral equation(4) can be solved by Wrench method[9] where equation is derived in algebraic form. Since the two propellers are moving relatively, the mutually-induced velocity varies with time, the mutually-induced velocity in calculation is the average value and can be found from Hough method[10].

$$\vec{u}(i) = \frac{1}{4\pi} \sum_{j=1}^m \Gamma_f(j) \cdot \vec{u}'(i,j) \quad (3)$$

$$\vec{u}'(i,j) = \int_0^\infty \frac{d\vec{l}(j) \times \vec{S}(i,j)}{|\vec{S}(i,j)|^3} \quad (4)$$

$$\Gamma_f(j) = -\frac{\Gamma(j+1) - \Gamma(j)}{\Delta r} \quad (5)$$

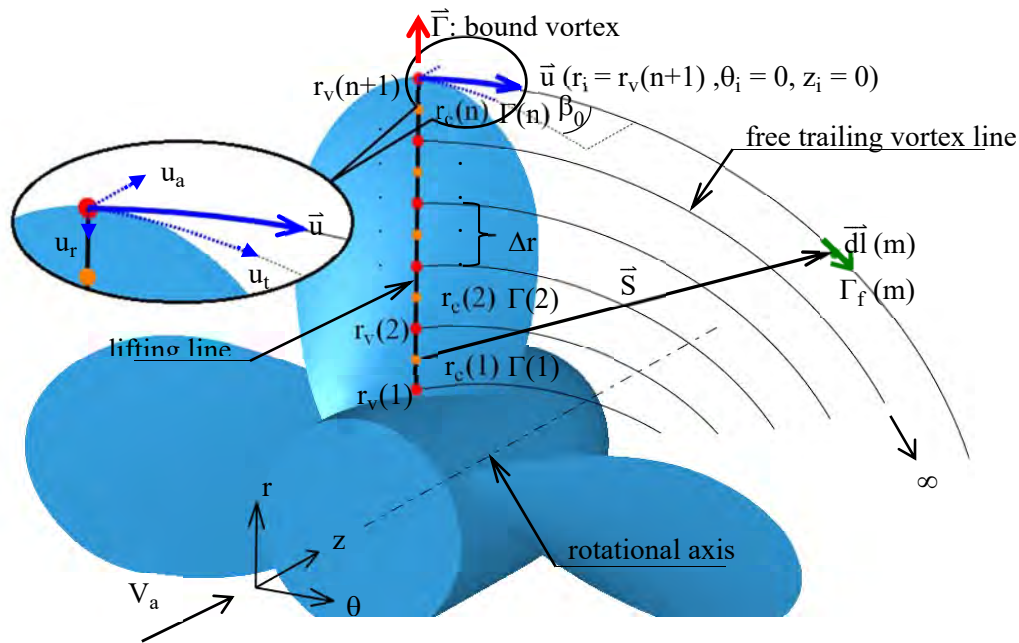


Figure1. Lifting line theory applied on propeller's blade.

2.2 Hub effect

Neglecting the hub effect causes the circulation at the blade root is to be zero but in reality there is load occurred on the blade root which means that the circulation does not vanish. This is caused by the present of hub. Kerwin and Leopold[11] proposed circulation distributing inside hub and also free vortex shed in downstream like blade's lifting line. The circulation is located at the image radius which is related to the radius of vortex point on lifting line as shown in equation(6). The pitch angle of hub free vortex line is found by equation(7). The circulation at image radius is equal to the circulation at correspond radius on lifting line but in opposite direction as shown in figure 2. The induced velocity caused by hub circulation is also found by Hough method[10].

$$r_{\text{image}(i)} = \frac{r_h^2}{r_v(i)} \quad (6)$$

$$\tan \beta_{\text{image}(i)} = \frac{r_v(i)}{r_{\text{image}(i)}} \tan \beta_0(i) \quad (7)$$

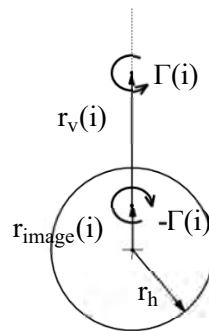


Figure 2. Vortex circulation inside the hub.

2.3 Slipstream contraction

Since flow that passes the propeller has cross section area decreased due to the increase in velocity, then the cross section is at first decreasing and becomes constant at a certain point downstream. The decrease of flow's cross section area or slipstream contraction results in the direction of free trailing vortex and also the induced velocity.

Owing to slipstream contraction, the free trailing vortex can be divided into two parts; transition and ultimate zone. The zone that cross section area starts decreasing in the beginning is called transition zone, and the zone that cross section area becomes constant is called ultimate zone. Hoshino[7] did propeller's open water test at different advance ratios and used the LVD to measure the radius of free trailing vortex. The measured vortex radius was summarized and represented by equations. The Hoshino's equations are applied to find free trailing vortex's radius with the assumption that free trailing vortex had been shed from the lifting line and the pitch angle of free trailing vortex line is constant. The free trailing vortex's radius is found from equation(8) to (14) where parameters in those equations can be explained by figure 3.

$$r_t(n,z)=r(n)-[r(n)-r_w(n)]\cdot f_r(\xi) \quad (8)$$

$$f_r(\xi)=\sqrt{\xi}+1.013\xi-1.920\xi^2+1.228\xi^3-0.321\xi^4 \quad (9)$$

$$\xi=\frac{z}{2.0R} \quad (10)$$

$$r_{wt}=[0.887-0.125(1-J/p)]R \quad (11)$$

$$r_{wh}=0.1R \quad (12)$$

$$J=\frac{\pi V_a}{\omega R} \quad (13)$$

$$p=2\pi\cdot 0.7R\cdot \tan(\beta) \quad (14)$$

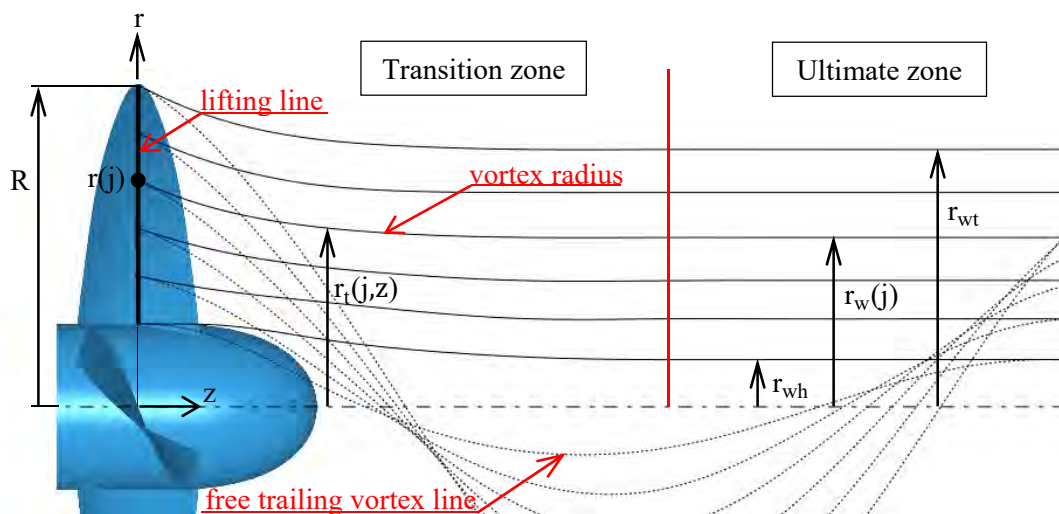


Figure 3. Slipstream contraction and parameters for calculating free trailing vortex's radius.

The self and mutually-induced velocity due to free trailing vortex in the ultimate zone can be found by Wrench and Hough's method respectively, whereas induced velocity due to free trailing vortex in transition zone cannot be found by these methods because its radius is not constant. However for transition zone occurred in finite distance, the induced velocity can be determined by applying the numerical method expressed in Biot-Savart law.

2.4 Calculus of variation method

According to Biot-Savart law and Jourovski's theorem, thrust and torque that developed by contra-rotating propellers depend on bound vortex circulation that distributed on both propellers. Finding appropriate circulation distribution definitely leads to a good result.

Coney[5] showed the way to find optimum circulation of various types of ship propulsion by using the calculus of variation method. For contra-rotating propellers, the optimum circulations under minimum power condition at required thrust (T_{req}) can be found by setting proper auxiliary function as shown in equation(15) and by solving set of equations that obtained from differentiating auxiliary function with respect to unknown circulations and Lagrange multipliers as shown in equation (16) to (19).

$$H=(\omega_1 Q_1 + \omega_2 Q_2) + \lambda_T (T_1 + T_2 - T_{req}) + \lambda_Q (Q_2 - q Q_1) \quad (15)$$

$$\frac{\partial H}{\partial \Gamma_1(i)} = 0 \quad \text{for } i=1,2,\dots,n_1 \quad (16)$$

$$\frac{\partial H}{\partial \Gamma_2(j)} = 0 \quad \text{for } j=1,2,\dots,n_2 \quad (17)$$

$$\frac{\partial H}{\partial \lambda_T} = 0 \quad (18)$$

$$\frac{\partial H}{\partial \lambda_Q} = 0 \quad (19)$$

3. Calculation procedure

To find the optimum circulation for contra-rotating propellers, relevant equations are programmed by using MATLAB program. The program is written under assumption that the free trailing vortex is shed from the lifting line and has constant pitch along the axial direction. The viscous force and hub drag are neglected and the incoming flow is uniform and in axial direction only. Since equations in calculus of variation method are non-linear, The Newton-Raphson iteration is applied to find optimum circulations by first assuming initial circulations and induced velocities as design parameters in the program. The radius of aft propeller is set to equal to radius of free trailing vortex tip at the distance where the aft propeller is located. The radius of aft propeller is varied due to induced velocity in each iteration as well as the shape of free trailing vortex lines. The iteration is continue until the circulation values are converge. The calculation procedure is shown in figure 4.

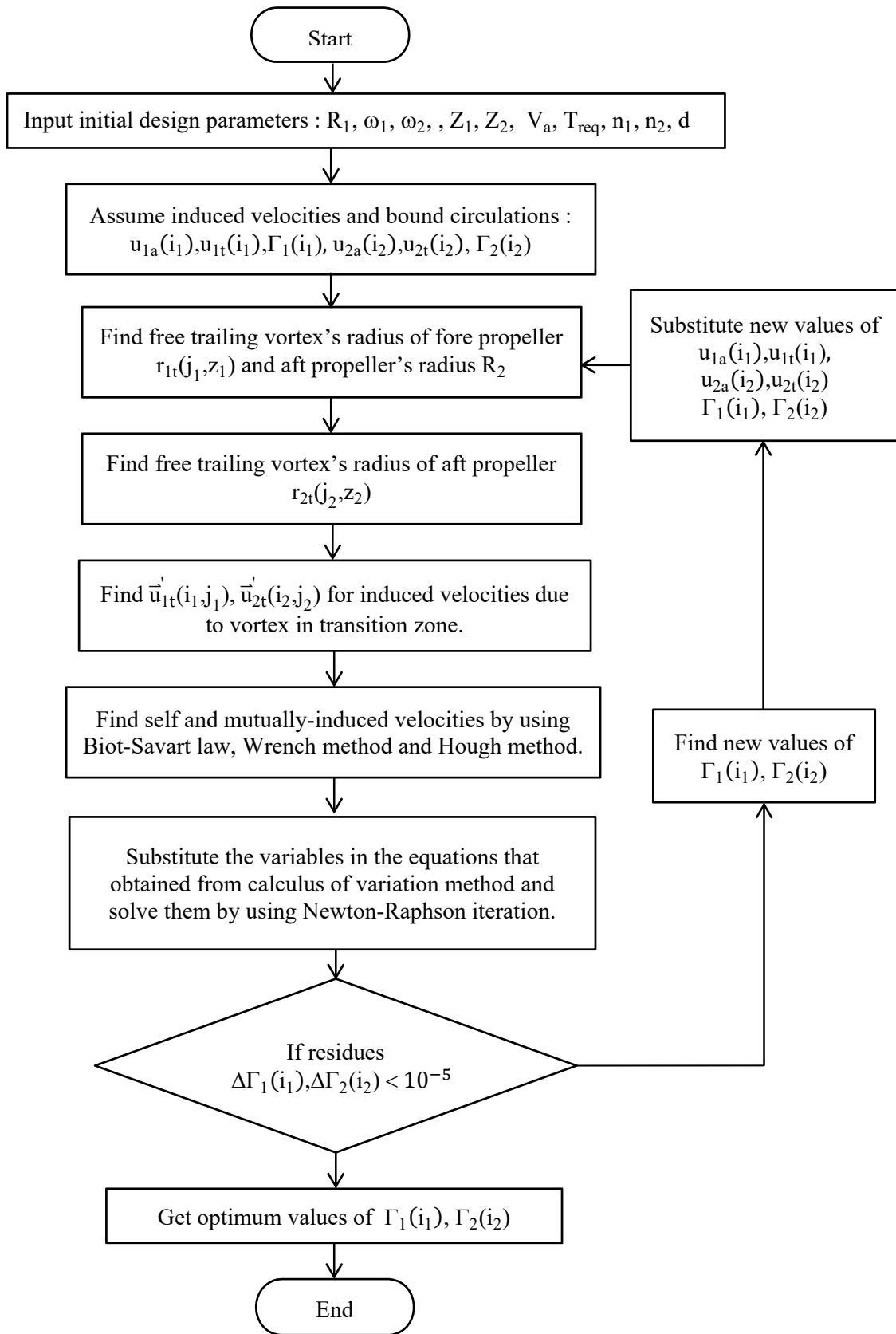


Figure 4. Flow Diagram showing the calculation procedure.

4. CFD analysis

4.1 Drawing propellers

Propeller with airfoil cross section can provide a better thrust on it. This thrust depends on type of airfoil, chord length, flow velocity and the angle between flow velocity and chord line which is called angle of attack as shown in figure 5.

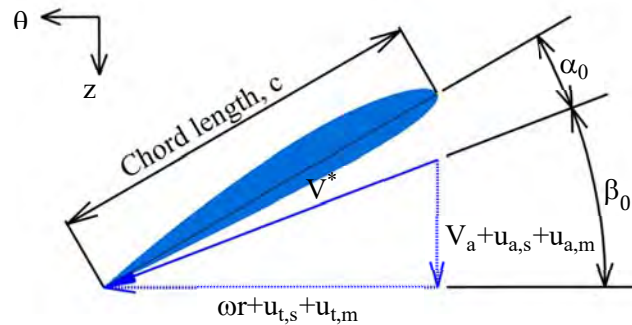


Figure 5. The alignment of cross section airfoil.

To draw the propeller's shape from circulations, type of airfoil and chord length have to be chosen first, then lift coefficient and angle of attack of each blade sections can be determined. The lift coefficient of any blade sections is found by substituting the circulation and the specified chord length at that blade section in equation(20). The lift coefficient is used to indicate the angle of attack by using the study of Abbott and Doenhoff[8] which shows the relation between the angle of attack and lift coefficient for various types of airfoil.

$$C_L(i) = \frac{2\Gamma(i)}{c(i).V^*} \quad (20)$$

Chord distribution is developed according to the distribution in the study of Oossanen[12] for each propeller with its developed area ratio at 0.5. The NACA2412 airfoil profile is chosen for blade cross section profile. The blade of propeller developed has no rake and skew angle to avoid the complication in applying correction factors for angle of attack.

4.2 CFD simulation

FLUENT Ansys program is chosen to simulate contra-rotating propellers that resulted from calculation. These propellers are simulated under same conditions in calculation procedure. The simulation uses sliding mesh method to determine results in each time step and k- ω model. The k- ω model gives good predicted results when compared with open water test results as shown in many studies such as Rhee and Joshi[13] and Kawamura[14]. The simulated model is shown in figure 6. The flow domain enclosing CRPs is modeled as cylinder shape with its radius and length equal to 1.3 and 3.5 times the fore propeller's radius respectively. Due to complex geometry of propeller, the unstructured mesh and refinement near blade and hub surfaces are applied. The flow is divided into two parts; one enclosed the fore propeller and the other covered both the aft propeller and the rest of flow domain. The interface surface of these two parts is in the middle between these two propellers where propellers and their hub start rotating in opposite direction. By this method, propellers can rotate relatively and move into a new position at each time step. Computational results at different relative positions in each time step can be obtained. The time step is chosen to give ten different relative positions between fore and aft propeller in each revolution.

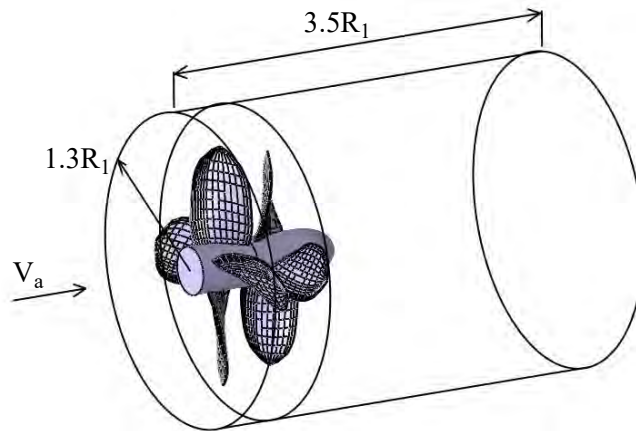


Figure 6. The domain of simulated CRPs.

5. Calculation and CFD results

The calculation is calculated at design parameters as shown in table 1.

Table 1. the input design parameters

parameter	value
T_{req}	3399.4236 [N]
V_a	2.05778 [m/s]
R_1	1 [m]
$\omega_1 = \omega_2$	6.4647 [rad/s]
d	0.45 [m]
$Z_1 = Z_2$	4
$n_1 = n_2$	10

From calculation, the optimum circulation distributions for each propeller are shown in figure 7.

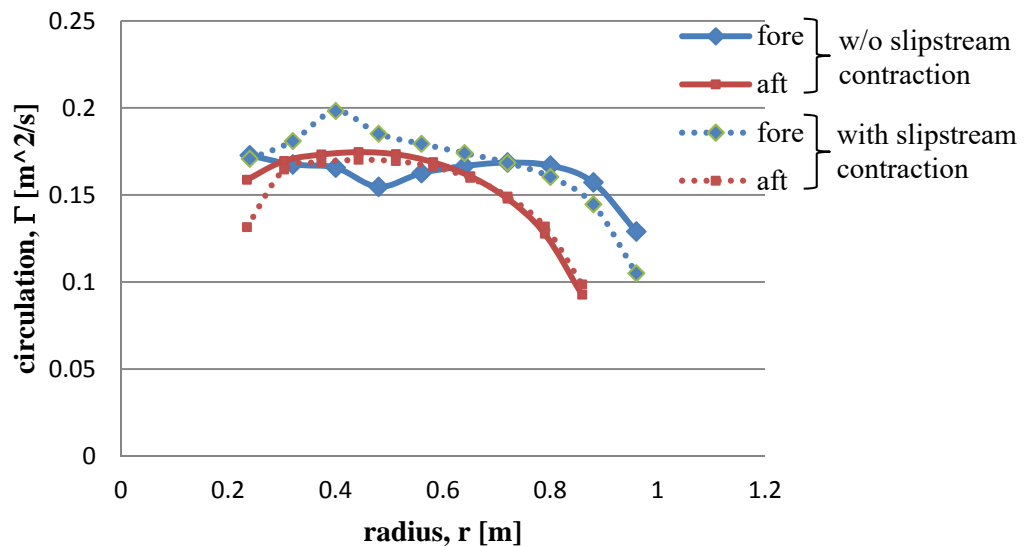


Figure 7. Optimum circulation distribution.

In the figure 7, results for circulation distribution obtained from CFD are then compared with those obtained from calculation without slipstream contraction effect condition. The difference between

cases that with and without slipstream contraction is the circulation on fore propeller. For fore propeller under slipstream contraction, strengths of circulation near the blade root tend to increase, while those at the blade tip tend to decrease when compare with circulations resulted from without slipstream contraction. This is resulted from slipstream contraction which pushes free trailing vortex lines to move inside the blade root and intensifies the strength of circulation at that area. While the difference in aft propeller is much smaller.

Thrust and torque obtained from calculation under with and without slipstream condition are shown in table 2. Both thrust and torque obtained are nearly the same because required thrust and torque ratios between fore and aft propeller are considered as constrained design parameters.

Table 2. Thrust and torque from calculation under with and without slipstream contraction.

	with slipstream contraction		w/o slipstream contraction	
	Fore propeller	Aft propeller	Fore propeller	Aft propeller
Thrust [N]	1902	1497.2	1899.5	1498.1
Torque [N.m]	699.56	559.64	697.13	557.70

The optimum circulation distribution that obtained from calculation under slipstream contraction condition is used to determine the section lift coefficient and to draw the propellers' blade profile. The drawn CRPs are simulated by FLUENT program as mentioned in section 4.2. The CRPs are calculated and simulated at condition mentioned in table 1 with two different rotational speeds, 6.4647 and 5.3873 rad/s which correspond to advance ratio 1 and 1.2 respectively. The viscous force is then included into thrust and torque obtained from calculation as shown in table 3 and 4 in order to compare with results obtained from FLUENT. This viscous force on each blade section is determined from the study of Abbott and Doenhoff[8].

From table 3 and 4, it shows that results obtained from calculation and FLUENT are different in term of value but are in the same order on fore and aft propeller. Consider as a single unit of CRPs, the total thrust and torque obtained from both calculation and FLUENT are also nearly same values as shown in table 5.

Table 3. Average thrust on fore and aft propeller.

Advance ratio	Thrust on fore propeller [N]			Thrust on aft propeller [N]		
	Cal.	Fluent	% Δ	Cal.	Fluent	% Δ
1	1,851.12	1,815.45	-1.93	1,456.18	1,541.07	3.22
1.2	1,817.89	1,677.97	-7.70	1,498.28	1,457.78	-2.70

Table 4. Average torque on fore and aft propeller.

Advance ratio	Torque on fore propeller [N.m]			Torque on aft propeller [N.m]		
	Cal.	Fluent	% Δ	Cal.	Fluent	% Δ
1	749.79	773.93	5.83	595.43	636.22	6.85
1.2	877.42	838.03	-4.49	700.88	694.40	-0.94

Table 5. Total thrust, total torque and efficiency of CRPs as a single unit.

Advance ratio	Thrust [N]			Torque [N.m]		
	Cal.	Fluent	% Δ	Cal.	Fluent	% Δ
1	3,307.30	3,356.53	1.49	1,345.22	1,410.15	4.83
1.2	3,316.18	3,135.75	-5.44	1,511.39	1,532.43	-2.91

6. Conclusion

Optimum circulation distribution of CRPs is determined by using lifting line theory and calculus of variation method. The lifting line and circulation distributing on it represent propeller's blade and the load occurring along the blade section. Equations are solved numerically by dividing the lifting line into finite elements with finite circulation strength. Induced velocities on each propeller are caused by its free trailing vortex in slipstream and the bound and free trailing vortex of the other propeller. Both vortex circulation strength and its direction affect the induced velocity and loads on propeller's blade, thus slipstream contraction is applied to lifting line theory to define the direction of free trailing vortex line. By using calculus of variation method, optimum circulation distribution that resulted in required thrust and minimum power usage on CRPs is found. The calculation results show that optimum circulation distribution under slipstream contraction tends to increase in area around blade root and decrease in area around blade tip when compared with results that neglect slipstream contraction.

The optimum circulation distribution under slipstream contraction condition is then used to determine the propeller's blade profile. This optimum blade profile is drawn and simulated in CFD program (Ansys FLUENT) to validate the calculation results. Results obtained from FLUENT show that thrust and torque on fore propeller as well as thrust on aft propeller are close to calculation results. This shows that calculation procedure, which based on lifting line theory and calculus of variation method along with the slipstream contraction condition, can provide a good approximate optimum design for CRPs. However this study has to be studied further at different condition such as at different advance ratio and required thrust in order to investigate a range of use or limitation of the design procedure.

nomenclature

c	chord length of blade cross section
C_L	Lift coefficient on blade cross section
d	Distance between fore and aft propeller
D	Propeller diameter
H	Auxiliary function
J	Advance ratio
dl	Infinitesimal of vortex element
n	Number of lifting line's element
p	pitch
q	torque ratio of aft propeller's torque to fore propeller torque
Q	Torque
R	Propeller radius
r_c	Radius at control point
r_h	Hub radius
r_{image}	Image radius inside the hub
r_t	Radius of free trailing vortex in transition zone
r_v	Radius at vortex point
r_{wh}	Radius of hub free trailing vortex in ultimate zone

r_{wt}	Radius of tip free trailing vortex in ultimate zone
Δr	Length of lifting line's element
S	Distance from control point to vortex
T	Thrust
T_{req}	Required thrust
u	Induced velocity
u'	Induced velocity coefficient
V_a	Axial velocity of incoming flow
V^*	Resultant velocity on blade cross section
Z	Blade number
α	Angle of attack
β_0	Pitch angle of free trailing vortex line
ρ	Flow density
Γ	Bound vortex circulation
ω	Rotational velocity
λ_T	thrust Lagrange multiplier
λ_Q	torque Lagrange multiplier

Subscript

1	The fore propellers
2	The aft propellers
r	Radial direction
t	Tangential direction
a	Axial direction
s	Self-induced value
m	Mutually-induced value

References

- [1] Lerbs H W 1952 *Moderately loaded propellers with a finite number of blades and arbitrary distribution of circulation* The society of naval architects and marine engineers (New York)
- [2] Lerbs H W 1955 *Contra-rotating optimum propellers operating in a radially non-uniform wake* David Taylor Model Basin **941**
- [3] Gunsteren L A 1973 *Application of momentum theory in counter-rotating propeller design* International Shipbuilding Progress **18**
- [4] Caster E B and LaFone T A 1975 *A computer program for the preliminary design of contrarotating propellers* David W. Taylor naval ship research and development center **SPD-596-01**
- [5] Coney W B 1992 *Optimum circulation distributions for a class of marine propulsors* Journal of ship research No.3 **36** pp 210-222
- [6] Laskos D 2010 *Design and cavitating performance of contra-rotating propellers* M.S. thesis Dept. Mech. Eng. MIT (Cambridge MA)
- [7] Hoshino T 1989 *Hydrodynamic analysis of propellers in steady flow using a surface panel method* J.S.N.A. (Japan) **165-166**
- [8] Abbott I H and Doenhoff A E 1959 *Theory of wing section including a summary of airfoil data* General Publishing Company Ltd.(Toronto Ontario)
- [9] Wrench J W 1957 *the calculation of propeller induction factors* Applied mathematics laboratory research and development **1116**
- [10] Hough G R and Ordway D E 1964 *The generalized actuator disk* The 2nd Southeastern Conf. on theoretical and applied mechanics (Atlanta Georgia)
- [11] Kerwin J E and Leopold R 1964 *A design theory for subcavitating propellers* The society of naval architects and marine engineers (New York)

- [12] Oossanen P 1974 *Calculation of performance and cavitation characteristics of propellers including effects of non-uniform flow and viscosity* NSMB Publication **457**
- [13] Rhee S H and Joshi S 2003 *CFD validation for a marine propeller using an unstructured mesh based RANS method* Proc.FEDSM '03 (Honolulu)
- [14] Kawamura T, Watanabe T, Takekoshi Y, Maeda M and Yamaguchi H 2004 *Numerical simulation of cavitation flow around propeller* J Soc of Naval Arch of Japan **195**